Visual Signal Pathway Reorganization in the *Cacna1f* Mutant Rat Model

Ye Tao,[1–3] *Tao Chen,*[1,3] *Bei Liu,*[4] *Jun Hui Xue,*[1] *Lei Zhang,*[1] *Feng Xia,*[1] *Ji-jing Pang,*[*,2] *and Zuo Ming Zhang*[*,1]

Purpose. To elucidate the underlying pathologic mechanism of congenital stationary night blindness (CSNB) by examining the characteristics of electrical signal transmission within the inner retinal circuit after *Cacna1f* gene mutation.

Methods. Retinas isolated from the spontaneous *Cacna1f* mutant rats or wild-type rats were placed into a recording chamber, with the ganglion cell layer facing the biochip electrode array. The light-driven responses of the retinal ganglion cells (RCGs) were recorded using a multielectrode array (MEA) system. In the electrical stimulus cases, charge-balanced biphasic current pulse trains were generated and applied to the central electrode of MEA to stimulate the RCGs. Chemical compounds were bath-applied through an active perfusion system. The acquired data were further analyzed off-line.

Results. Typical electrical responses were successfully recorded in the retinas of both wild-type rats and *Cacna1f* gene mutated rats. In the *Cacna1f* mutant retinas, the amplitude of the light-induced a-wave was decreased, paralleling the vanished b-wave. The responsive a-wave was not blocked by the application of 100 μM 2-amino-4-phosphobutyric acid. The increased spontaneous firing rate and the decreased robustness of light-driven signaling reflected a loss in the ability of ganglion cells to encode visual signals reliably and economically. Moreover, the ON pathway is somehow disconnected from ganglion cells, whereas OFF pathways may be preferentially selected by the CSNB retinas. In the electrical stimulus cases, the long-latency responses of RGCs evoked by the indirect synaptic inputs from outer layers of retina were weaker in the CSNB rats compared with that of SD rats.

Conclusions. Using MEA recording, we provide evidences of functional changes for visual signal pathway plasticity in the *Cacna1f* mutated retinas. Our results suggest that the dysfunctions in photoreceptor neurotransmitter release and the loss of signaling efficiency both occur during CSNB, and the latter is possibly reversible. (*Invest Ophthalmol Vis Sci.* 2013;54:1988–1997) DOI:10.1167/iovs.12-10706

Calcium ion influx through L-type voltage-gated channels activates the readily releasable pool in the presynaptic ribbon terminals of photoreceptors and triggers off neurotransmitter exocytosis.[1–4] This is the key biological process in visual signal generation and transmission.[5–7] These functional L-type currents are predominantly attributable to the Cav1.4 channel in mammalian retina.[8,9] Several mutations within *Cacna1f*, the gene that codes for the α1f subunit of the Cav1.4 calcium channel, impair the rod signal pathway and the cone signal system. These mutations are also associated with incomplete X-linked congenital stationary night blindness (iCSNB), a hereditary form of severe night vision loss.[9–12] Defects in the α1f subunit have been reported to cause abnormalities in number, structure, and function of photoreceptor ribbon synapses and, consequently, interrupt synaptic transmission from photoreceptor to second-order neurons in nob2 mice.[13,14]

The CSNB rats with mutated *Cacna1f* gene have the electroretinogram (ERG) phenotype that closely resembles that of the iCSNB patients.[12,15,16] Therefore, this spontaneously mutated animal model is of particular importance in pathophysiologic studies on iCSNB. A recent morphologic study found that bipolar cells in the *Cacna1f* mutant rat's retina exerted ectopic synapses to the outer laminae of the outer nuclear layer (ONL). Study of the *Cacna1f* mutant rat also showed a decrease in the thickness of the outer plexiform layer (OPL) and the number of horizontal cells, whereas the microstructure of the inner retina seemed relatively intact and consolidated.[17] These impressive rectifications of outer synaptic inputs likely affect the inner retinal circuits. However, little is known about the physiologic effects on the ultimate action potential signals of retinal ganglion cells (RGCs).

The multielectrode array (MEA) system has been used in the retinal studies.[18–20] A special map of neural electrophysiologic functions and retinal network activities can be drawn by simultaneously acquiring the electrical response of various retinal locations from as many as 64 electrodes, providing valuable clues for the intercellular "talks" within inner retinal circuits. Due to its ensemble and noninvasive advantages, this technology bridges the gap between the conventional in vitro recording and the complicated in vivo recording, especially in electrophysiologic explorations that target ion channels.[19,20] The MEA system has been adopted for recording the activities of retinal neurons such as ganglion cells[21–23] and photoreceptors.[18,24] Using this instructive recording system and the

From the [1]Department of Clinical Aerospace Medicine, Fourth Military Medical University, Xi'an, People's Republic of China; the [2]Department of Ophthalmology, University of Florida College of Medicine, Gainesville, Florida; and the [4]Department of Neurosurgery and Institute for Functional Brain Disorders, Tangdu Hospital, Fourth Military Medical University, Xi'an, People's Republic of China.

[3]These authors contributed equally to the work presented here and should therefore be regarded as equivalent authors.

Supported by Nature Science Foundation of China Grants 30872838 and 30571999.

Submitted for publication August 4, 2012; revised October 22 and December 29, 2012 and February 8, 2013; accepted February 14, 2013.

Disclosure: **Y. Tao**, None; **T. Chen**, None; **B. Liu**, None; **J.H. Xue**, None; **L. Zhang**, None; **F. Xia**, None; **J. Pang**, None; **Z.M. Zhang**, None

*Each of the following is a corresponding author: Zuo Ming Zhang, Department of Clinical Aerospace Medicine, Fourth Military Medical University, Xi'an, People's Republic of China; zhangzm@fmmu.edu.cn.

Ji-jing Pang, Department of Ophthalmology, University of Florida College of Medicine, Gainesville, FL 32610; jpang@ufl.edu.

Investigative Ophthalmology & Visual Science, March 2013, Vol. 54, No. 3

spontaneously mutated CSNB rats, the modified physiologic properties of the visual signal pathway in the iCSNB retina and the underlying pathologic mechanisms of retinal remolding were explored in the present study.

Methods

Animals

All experiments were performed in accordance with the ARVO Statement for the Use of Animals in Ophthalmic and Vision Research. The spontaneous gene mutant rats were obtained from the 23rd inbred generation that derived from the originally identified mutant rat,[12] whereas the wild-type (Wt) rats (Sprague-Dawley) were provided by the Laboratory Animal Research Center of the Fourth Military Medical University. All animals were maintained under standard laboratory conditions (18–23°C, 40%–65% humidity, 12-hour dark/light cycle) with food and water available without restriction.

Tissue Preparation and MEA Recording

The 8- to 10-week old Wt and *Cacna1f* mutant rats were dark-adapted overnight before recording. The animals were euthanized by quick cervical dislocation under dim red light. The eyes were enucleated and dissected immediately. The neural retina was gently removed from the pigment epithelium layer of the eyecup and placed into the recording chamber, with the ganglion cell layer facing the MEA biochip electrode array. The electrode array used in the present study contains 64 electrodes, arranged in an 8×8 layout with 450 or 100 μm for space configuration (Alpha MED Sciences Ltd., Osaka, Japan). A nylon mesh and a slice anchor were then placed over the retina to hold it in place. A small drop (5.0 μL) of cellulose nitrate solution (1.0 mg Sartorius-scaled cellulose nitrate dissolved in 10.0 mL methanol; Sartorius AG, Goettingen, Germany) was smeared on the electrode array as electric glue to ensure better retinal contact. Two kinds of electrodes with different dimensions were used: (1) the bigger electrode array (electrode diameter, 50 μm) was used for field potential recording to attain a global convergence of retinal neurons' chorus; (2) the smaller electrode array (electrode diameter, 20 μm) with better spatial sampling ability and higher sensitivity was used to record the firing spikes and the cross-correlations of RGCs (Fig. 1).

During recording, the retina samples were perfused with oxygenated Ringer's solution (95% O_2 and 5% CO_2) for mammalian retinas (containing the following [in mM]: 124 NaCl, 5 KCl, 25 $NaHCO_3$, 2.5 $CaCl_2$, 1.15 $MgSO_4$, 1.15 KH_2PO_4, and 10 D-glucose) at a flow rate of 1 mL/min. To obtain stable data, the light response of the retinal ganglion cells was recorded after 1 hour of adaptation to the solution environment.

The chemical compounds were bath-applied through an active perfusion system. Tetrodotoxin (TTX), 2-amino-4-phosphonobutyric (APB), *cis*-2,3-piperidinedicarboxylic acid (PDA), 18β-glycyrrhetinic acid (18β-GA), and 6-cyano-7-nitroquinoxaline-2,3-dione (CNQX) were obtained from Sigma (St. Louis, MO). The responses were recorded using the MEA system (MED-64; Alpha MED Sciences Ltd.). The analog extracellular neuronal signals from 64 channels were AC amplified, sampled at 20 kHz, and stored on a compatible computer for subsequent off-line analysis. All recordings were subsequently subjected to off-line spike sorting and analysis using commercial software (Offline Sorter; Plexon Inc., Dallas, TX; and Neuroexplorer; Nex Technologies, Littleton, MA).

Stimulus and Spike Analysis

The responses were elicited by white light–emitting diodes (LEDs).The generated light was projected onto the retinal surface via a lens focus system, at a mean photonic intensity of 950 mcd·s/m^2. The LEDs were driven by a computed stimulator to provide the retina a uniform full-field illumination.

Before spike detection, the field potentials were wiped off through a band-pass filter (100–3000 Hz). The threshold for spike detection was set to four times the SD of the mean value of the measured signal for each electrode.[19,20] These candidate spike waveforms were then sorted (Offline Sorter; Plexon Inc.). The clusters were first identified using a K-mean cluster algorithm, and then manually edited for clustering errors. The interspike interval (ISI) histograms were analyzed as described previously for each unit to determine the regularity and distribution of the spikes, and thereby to elucidate the cell firing pattern.[21] The peristimulus time histograms (PSTHs) and the raster plots of individual units were used to categorize the ganglions.[19,23] The units without visual response were categorized as nonresponsive. These units with a visual response, but showed no clear peaks at either stimulus onset or offset, were categorized as others. The PSTHs were smoothed using a Gaussian kernel to analyze the latency of the ON and OFF responses. The time from the onset or offset of light stimulus to the maximum peak was defined as the ON or OFF response latency.

The electrical stimulus was set as described previously.[25] In brief, charge-balanced biphasic current pulse trains were generated (anodic pulse first, no temporal separation between two phases) and applied to one electrode (No. 28) at the center to stimulate the RCGs.

The pulse amplitude and the duration were fixed at 30 μA and 500 μs, respectively, which reliably evoked the RGC responses. Each trial was repeated 10 times. The RGC response intensities were measured by counting the number of evoked spikes within 10 to 50 ms poststimulus. Each value was averaged from the 10 repeated stimulations.

Statistical Analysis

The clusters were first identified by a K-mean cluster algorithm. An unpaired Student's *t*-test was used on multifocal ERG recordings to assess the statistical differences between the *Cacna1f* mutant and Wt rats. In the MEA recording from RGCs, the statistical significance of the differences in mean firing rates and discharge patterns between *Cacna1f* mutant and Wt rats were calculated using a Kruskal–Wallis ANOVA, followed by the Kolmogorov–Smirnov test. $P < 0.05$ was considered significant. The values are presented as mean ± SEM, unless otherwise specified.

Results

Light-Induced Field Potentials

The isolated rat retinas were placed on the MEA with the RGC layer against the chip. Typical electrical responses of the Wt retinas were successfully elicited by the light from white LED and harvested by each MEA electrode (Fig. 2A): the a-wave, the main negative response after the light onset that represents the photoreceptor activity (0.196 ± 0.038 mV, $n = 20$); and the b-wave, the positive response immediately after the a-wave (found in 12 of a total 22 specimens). The c- and d-waves,[18] which were derived from pigment epithelium cells, were not recorded in the present study because the pigment epithelium layer was removed from tissue specimens. Application of 100 μM APB, a selective agonist of mGluR6 in ON-bipolar cells, blocked the responsive a-waves, but not b-waves (Fig. 2C). The insensitivity of the responsive a-wave to APB indicates its total dependence on the photoreceptor activity.[24]

In the *Cacna1f* mutated retinas, the light-induced a-waves can still be detected with significantly reduced amplitude when compared with those of Wt retinas (0.078 ± 0.026 mV, $n = 20$, Kruskal–Wallis test, $P < 0.01$, Fig. 2B), which suggested that the light-induced responses of photoreceptors were partly retained in the *Cacna1f* mutant retinas, and these photoreceptors were partly functional after *Cacna1f* mutation. However, no b-wave was recorded in any of the *Cacna1f*

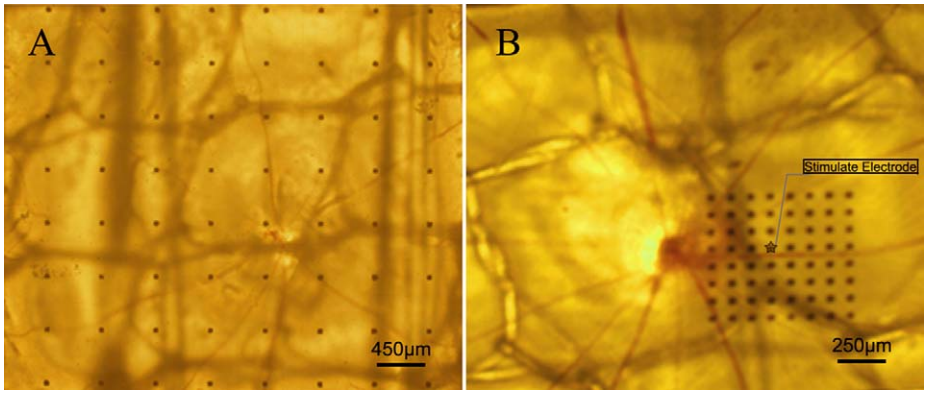

Figure 1. Two kinds of electrodes with different dimensions were used. (**A**) The bigger electrode array was used for field potential recording to attain global convergence of retinal neurons' signal. (**B**) The smaller electrode array was used for recording firing spikes and cross-correlations of RGCs to avoid the relatively coarse spatial sampling and the limited sensitivity of large electrode array. The stimulating electrode was marked.

mutant retinas, which implies a disruption of visual signal transmission between the photoreceptors and the ON-bipolar cells.

Electrical Stimulated Response

After electrical stimulation, spikes were recorded in 384 and 366 single RGC units from 10 sets of the Wt and *Cacna1f* mutated retinal patches. Reliable evoked responses were recorded in 147 and 131 of them and were eligible for further analysis. An example of the recorded waveforms of single RGC activities that responded to the stimulus pulses in the Wt and *Cacna1f* mutant rats is shown in Figures 3A and 3B. Two types of RGC responses were evoked by the electrical stimulus in the present study as previously reported.[26,27] The short-latency responses were evoked within 5 ms after stimulation, and the long-latency responses were evoked approximately 10 to 50 ms after stimulation. The short-latency responses were generated by direct stimulation of the RGCs, whereas the long-latency responses might be produced by indirect stimulation from the outer retina through synaptic communication. The response intensity of RGCs decreased as the distance between the stimulating electrode and recording electrode increased.[27] Therefore, the reliably responding RGCs were categorized into different subgroups based on the distance between the stimulating electrode and the recording electrode (distance [in μm]: 100, 141, 200, 223, 283, 300, 316, 361, 387, 400, 424, 447, 500, and 566). The number of evoked spikes within 10 to 50 ms poststimulus in each subgroup in the *Cacna1f* mutated rats was significantly lower than that in the Wt rats (Fig. 3C). These findings suggested that the long-latency responses decreased in the *Cacna1f* mutated rats.

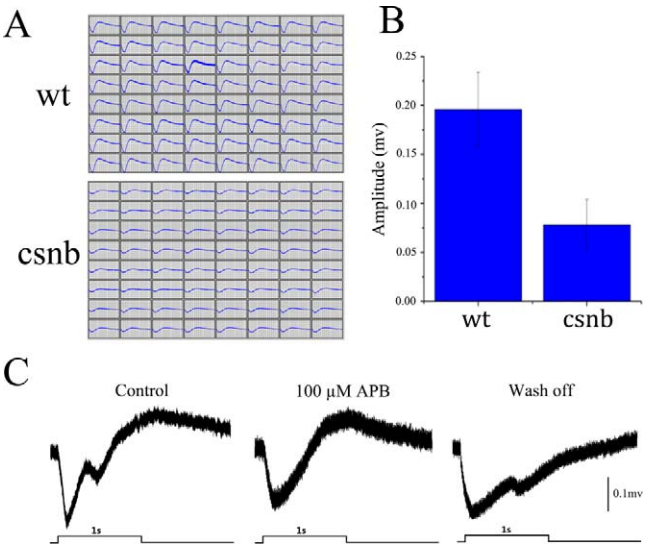

Figure 2. (**A**) Light-induced a-waves, the main negative response after light onset, which represented the activity of photoreceptors, were recorded in both Wt and *Cacna1f* mutant retinas. (**B**) The amplitude of the light-induced a-waves was decreased significantly in *Cacna1f* mutant rats compared with the Wt. (**C**) The b-wave, the positive response immediately after the a-wave in Wt retinas, was totally abolished by 100 μM APB, a selective mGluR6 agonist in ON-bipolar cells.

Spontaneous Spikes

The smaller electrode (20 μm) for recording the action potentials of RGCs was used to explore how the *Cacna1f* mutation affects the signal transmission in the inner retina. The MEA recording was used to monitor the spontaneous extracellular firing spikes from 30 to 90 RGCs simultaneously from each retina after dark adaptation and stabilization. The RGCs of the *Cacna1f* mutant retina fired at a much higher spontaneous frequency than did those of the Wt (Fig. 4A). It was observed that a single electrode occasionally detected activities from two or more RGCs. The activity of these multi-RGCs was excluded, to avoid potential missorting of spikes and to obtain more accurate measurements. Only recordings obtained from a single cell per channel were included in subsequent analysis.[21]

The rightward shift and decreased initial slope in the cumulative frequency histograms were observed in *Cacna1f* mutant retinas, indicating increased spontaneous firing rate of a larger RGC proportion (Fig. 4B). The quantitative analysis showed that the average frequency of spontaneous spikes was significantly higher in the *Cacna1f* mutant retina than that in the Wt retina (Kruskal–Wallis test, $P < 0.01$, Fig. 4C); Thus, spontaneous hyperactivity occurred in the inner retina as photoreceptors' function degenerated in the *Cacna1f* mutant retina.

This inclination could be exemplified by two representative pairs of RGCs from different Wt retinas and *Cacna1f* mutant retinas. As illustrated in the firing rate histograms (Fig. 4D), the average spike rate over a 50-second period in the *Cacna1f* mutant RGCs (cell 1 = 9.94 Hz, cell 2 = 15.01 Hz) was higher than that of the Wt RGCs (cell 1 = 2.13 Hz, cell 2 = 2.08 Hz)

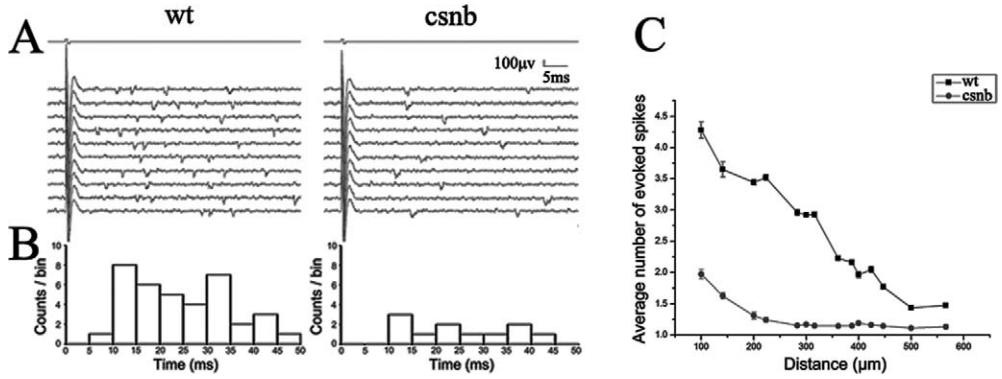

Figure 3. (**A**) The recorded traces of 10 repeated electric stimulations in the Wt (*left*) and *Cacna1f* mutant retinas (*right*). The stimulus pulse is shown at the *top*. (**B**) The poststimulus time histogram (constructed from 10 trials, bin size: 5 ms) of both Wt and *Cacna1f* mutant retinas. (**C**) The RGCs' response strength in both the Wt and *Cacna1f* mutant retinas decreased as the distance between the stimulating electrode and the recording electrode increased (*error bar* denotes SE).

Discharge Patterns of Spontaneous Spikes

The ISI histograms and autocorrelations analysis was used to evaluate the discharge patterns of the spontaneous firing RGCs in the present study[21,28,29]: regularly firing cells, exhibiting the normally symmetric distribution of intervals on ISI histograms; irregularly firing cells, showing ISI histograms with the asymmetric distribution; bursting cells, bursting with the no or single spike periods; and mixed cells, showing a random spike firing that superimposed on the burst. The majority (90.6%) of the detected RGCs ranked among these four typical subtypes (Fig. 5A). According to this classification, the proportions of bursting and mixed-type firing RGCs were significantly higher in the *Cacna1f* mutant retinas at the expense of a decrease in the proportion of irregularly firing RGCs (Fig. 5B). In addition, the total spike number of each RGC subtype was calculated. It was found that the spike number of the mixed-type RGCs was higher in the *Cacna1f* mutant retinas (246,553, $n = 20$) than that in the Wt retinas (112,089, $n = 20$, Kruskal–Wallis test, $P < 0.01$). The spike numbers of the other three RGC types were similar in both kinds of retinas ($P > 0.05$). Therefore, the mixed-type RGCs might be responsible for the spontaneous hyperactivity of the *Cacna1f* mutant retinas. Those ambiguous RGCs (9.4%), which could not be accurately attributed to any of the aforementioned types as the low-firing rate, were not included in our interpretation.

Light-Evoked Spikes and Correlated Activities

Full-field light flashes evoked responses in both the Wt and *Cacna1f* mutant retinas. The spikes were extracted from the underlying field potential with the pass frequency of 100 to 3000 Hz using off-line software (Spike Sorter; Plexon Inc.). The light-induced ON and OFF spikes were extinguished by 100 μM TTX (Fig. 6A), suggesting that they were the RGCs' action potentials triggered by visual signal inputs from the photoreceptors.

Using the formerly described classification method,[30,31] six main categories of RGCs from both central and peripheral retinal regions were identified by their response characteristics to light stimulus. These categories included: responding predominantly to light onset (ON), to light offset (OFF), or to both (ON–OFF); sustained response to light onset (sustained ON); sustained response to light on and offset (sustained ON–OFF); and sluggish response to light offset (delayed OFF). The PSTHs under raster plots also revealed the presence of these RGC populations in the *Cacna1f* mutant retinas (Fig. 6B). Other rarely encountered types were not included in our calculation.[31] These MEA data proved that the basic physiologic response types and a substantial part of RGCs' function were retained in the *Cacna1f* mutated retinas, despite the inputs from photoreceptors degraded and the morphology of OPL substantially changed.

The correlated activities between neighboring or distant RGCs were investigated to determine the circuit organization of the retinal network. In the *Cacna1f* mutant retinas, we observed two of the three cross-correlation characteristics of normal RGCs.[32] They were excitatory correlations with narrow-scale (<1 ms) and medium-scale (<25 ms) correlations, respectively (Figs. 7Aa, 7Ab). Such correlations at relatively short-scale intervals originated from the inner retina and they were mediated through gap junctions between the RGCs and/or the amacrine cells. These synchronous "talks" between RGCs suggested that the intercellular communication within the inner retinal network was well retained in the *Cacna1f* mutated retina. To dissect the role of these gap junctions, a potent gap junction blocker 18β–GA was applied in the Wt and the *Cacna1f* mutated retinas' discharging recordings. In the *Cacna1f* mutated retinas ($n = 5$), 100 μM 18β–GA caused a pronounced decrease in the firing frequency of spontaneous firing spikes, whereas no appreciated effect was found in any of the Wt retinas ($n = 5$, Fig. 7B). This difference indicated that gap junctions were closely related to the correlated electrical discharges and these gap junctions had been upregulated in the *Cacna1f* mutated rats after the disruption of visual signal transmission in the outer retina.

The RGCs pair displaying correlated activity at broad-scale intervals (40–100 ms) was not detected in any of the recorded *Cacna1f* mutated retinas. This correlated activity was commonly seen in the Wt retinas and could be eliminated by blocking the chemical synaptic inputs from photoreceptors (Fig. 7Ac). Given that the origin of these cross-correlations involved the participation of photoreceptors and bipolar cells in polysynaptic circuits,[32,33] the absent contribution of the polysynaptic inputs to RGCs' interactions was most likely disrupted by the malfunctioning L-type calcium channels, which might lead to disruption of chemical synaptic inputs.

Pathway Remolding of the Retinal Circuit

The ON and OFF responses were separated to find out the exact subtype of RGCs that would be responsible for the reduction in total responses of the *Cacna1f* mutant retinas. It was found that the ON responses degenerated disproportionately to the OFF responses, which remained relatively preserved in the *Cacna1f* mutated retinas (Fig. 6C). Therefore,

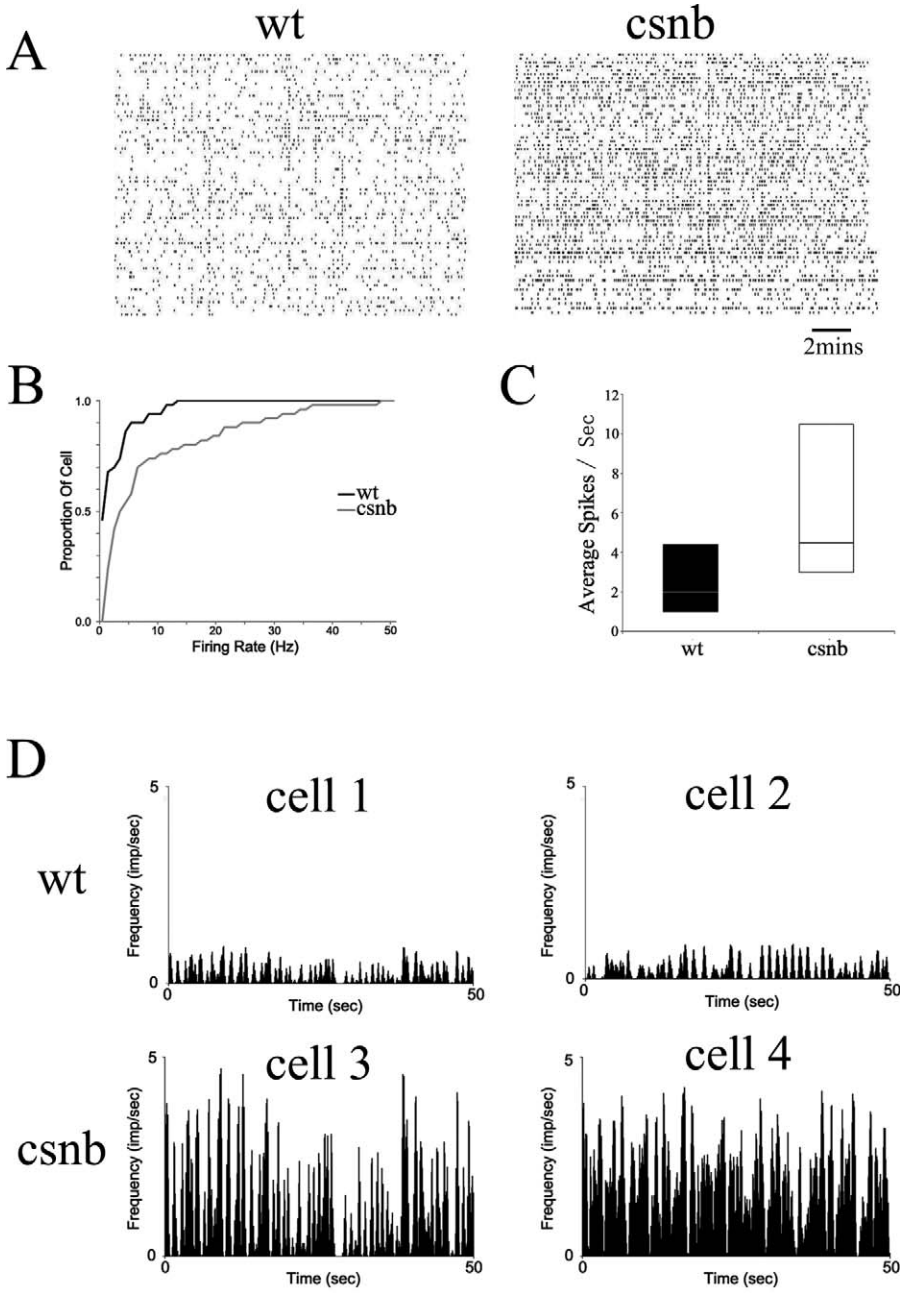

Figure 4. (**A**) Recorded neural activities of RGCs evoked by stimulus pulses. The raster plots indicated that the RGCs from the *Cacna1f* mutant retinas fired at a much higher spontaneous frequency than the Wt RGCs. (**B**) The increased firing activity could be found in a larger proportion of *Cacna1f* mutant RGC populations, compared with their Wt counterparts, demonstrated here as a rightward shift and decreased initial slope in the cumulative frequency histograms. (**C**) Detailed quantitative analysis of the elevation in the spontaneous activity in the *Cacna1f* mutant retinas demonstrated a statistically significant difference (Kruskal–Wallis test, $P < 0.01$, Fig. 2). (**D**) This inclination can be exemplified by two representative pairs of ganglion cells from two sets of Wt and *Cacna1f* mutant retinas.

this alteration in the total responses of *Cacna1f* mutant retinas could be attributed to the ON RGCs.

Considering their complex physiology, no widely accepted classification protocol was readily available for rat RGCs. Therefore, it is difficult to determine if the decrease in ON response was caused by alterations in a specific subtype of RGCs or overall cell populations. We delineated the distribution of these ganglion cells according to the relative proportion of ON versus OFF response amplitude that made up the total light response. Primarily, these ganglion cells were divided into ON-dominant (ratio > 0.5), OFF-dominant (ratio < 0.5), and equal (ratio $= 0.5$).[30,31] More OFF-dominant cells and fewer ON-dominant cells were found in the *Cacna1f* mutant retinas. The distribution of recorded firing spikes among such subgroups revealed that a significantly greater proportion of the entire cell population was dominated by OFF responses in the *Cacna1f* mutated retinas than that in the Wt retinas. The retinal ON and OFF signal pathways in the inner retina were differentially affected by *Cacna1f* gene mutation. These progressive modifications in the ON and OFF pathways could be considered a consequence of developing plasticity of the retina circuits after congenital gene mutation in the outer

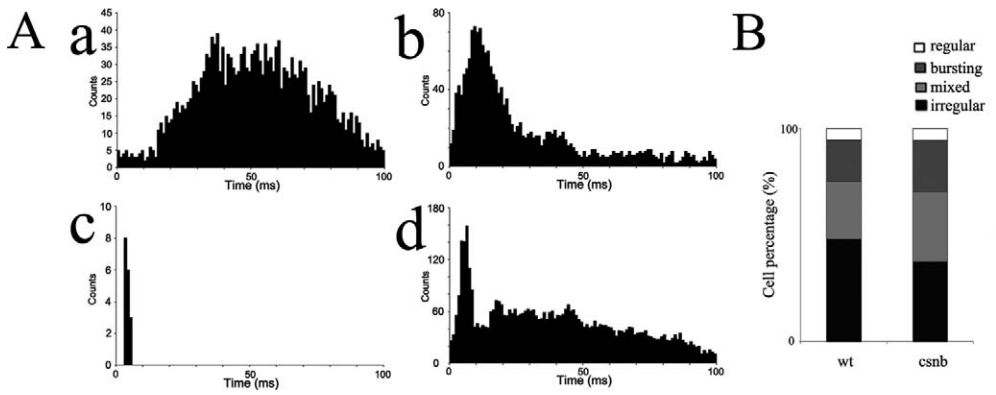

Figure 5. (**A**) Four typical discharge patterns based on their ISI histograms: bursting cells (**a**), regularly firing cells (**b**), irregularly firing cells (**c**), and mixed type cells (**d**). (**B**) Following this classification, the proportions of the bursting and the mixed types firing RGCs were found to be significantly increased in *Cacna1f* mutant retinas at the expense of the decreased irregularly firing RGCs.

retina. The latency of both the OFF and ON responses significantly increased in the *Cacna1f* mutant retinas (Kruskal–Wallis test, $P < 0.05$, Fig. 6D). The delay was consistent with the disappearance of the b-wave in the field potential of the *Cacna1f* mutant retinas, which implied the disruption of visual signal transmission between the photoreceptors and the ON-bipolar cells in the OPL. This interruption in the onset ON signal pathway caused pathway reorganization in the downstream neuron circuits.

Then 50 μM CNQX + PDA cocktail was applied to block the OFF signal pathway. The majority of OFF responses in both kinds of retinas were disrupted by the CNQX + PDA cocktail. The firing rate of total response decreased, whereas the firing frequency of the ON response increased in the *Cacna1f* mutated retinas (Fig. 6C, Blocked). In addition, the latency of ON responses was significantly increased in the *Cacna1f* mutant retinas after the application of CNQX + PDA cocktail (Fig. 6D, Blocked). In both kinds of retinas, the OFF responses of the OFF RGCs and the ON–OFF RGCs were disrupted by the CNQX + PDA cocktail, but the OFF responses of the delayed OFF RGCs and the sustained ON–OFF RGCs were not (Fig. 6B, Blocked). Therefore, the OFF firing spikes from the latter two RGC types constituted the residual OFF responses that were not blocked by cocktail.

Discussion

Most studies on CSNB focus on the anatomic changes and functional states of photoreceptors.[8–10,13] On the other hand, the functional changes in the inner RGCs after *Cacna1f* mutation have not been reported. The MEA system can systematically examine the electrophysiologic properties of neurons in *Cacna1f* mutated retinas.[18–20] Its electrodes have a high sensitivity for the subtle and focal activation of retinal neurons, probably because of their direct contact with retinal tissue. Given that it can detect the functional recovery in a local treated area, spatial MEA data should be of particular value in the therapeutic studies such as gene therapy and cell transplantation.[24]

Our MEA research identified marked alterations in the physiologic activity of retinal neurons that accompany visual signal pathway reorganization in a naturally mutated animal model. We profiled several pathologic features of iCSNB that have not been described previously. The presence of residual light-induced a-wave indicates that photoreceptors are partially functional in the *Cacna1f* mutant retinas. The disappearance of the b-wave, which mainly reflects ON-bipolar cell and Müller cell activity,[18] implies a disruption of visual signal transmission between the photoreceptors and the ON-bipolar cells in *Cacna1f* mutant retinas. The b-wave was not recorded from several Wt retinas (10 of 22). It is unstable in MEA recording and corresponds to the b-wave of traditional ERG.[18,24] The b-wave, which is smaller in the recordings from isolated retinas than in recordings from intact eyes,[18] may also be eliminated by perfusion with changes in ionic balance[34,35] or by the blockage of blood flow in laboratory animals[36] and in human patients.[37] These factors may be the cause of instability of b-waves in Wt retinas and in electrical stimulation, the long-latency responses fired at a lower frequency in *Cacna1f* mutant retinas. The dysfunction of the L-type calcium channel causes disturbances in retinal signal transmission. Under such a condition, although the neurons in the outer layer of retina are stimulated by electrical current, the generated signals could not be transmitted to RGCs through synapses. Therefore, the lower firing frequency of long-latency responses proves that the indirect synaptic inputs from the outer retina are affected by *Cacna1f* mutation.[25,27]

Given that the relatively minimal contribution of RGC activity makes to the full-field ERG,[38,39] the present study first describes the inner retinal function alterations of the CSNB animal model. These discharge patterns of spontaneous activity together with the light-stimulated responses recorded in the present study are typical in mammalian RGC physiology, thereby validating our recording conditions.[30,40–43] The spontaneous hyperactivity found in CSNB rats' retinas suggests a significant alteration in the electrophysiologic properties after *Cacna1f* mutation. Considering the trivial expression of the *Cacna1f* gene in the inner retina, mutation of this gene is unlikely to alter the intrinsic cellular function of the RGCs, such as membrane properties, dominant receptive fields, and so on.[10] A more likely mechanism underlying this hyperactivity might be attributed to various alterations in the organization of inner retinal circuits that are presynaptic to the RGCs. The cause might be the abnormal excitatory versus inhibitory imbalance, which is based on the increased glutamatergic inputs and/or decreased inhibitory GABAergic inputs to RGCs.[44–46]

Further separate examination of the ON and OFF responses showed that the interruption of visual signal transmission between the photoreceptors and the ON-bipolar cell causes pathway rearrangement in downstream neuron circuits: the ON pathway was somehow disconnected with RGCs, whereas the OFF pathway might be preferentially selected by the *Cacna1f* gene mutated retina; the lower total firing rate of the light-induced response in *Cacna1f* mutant retinas can mainly be attributed to the aggressive loss of the ON response. These

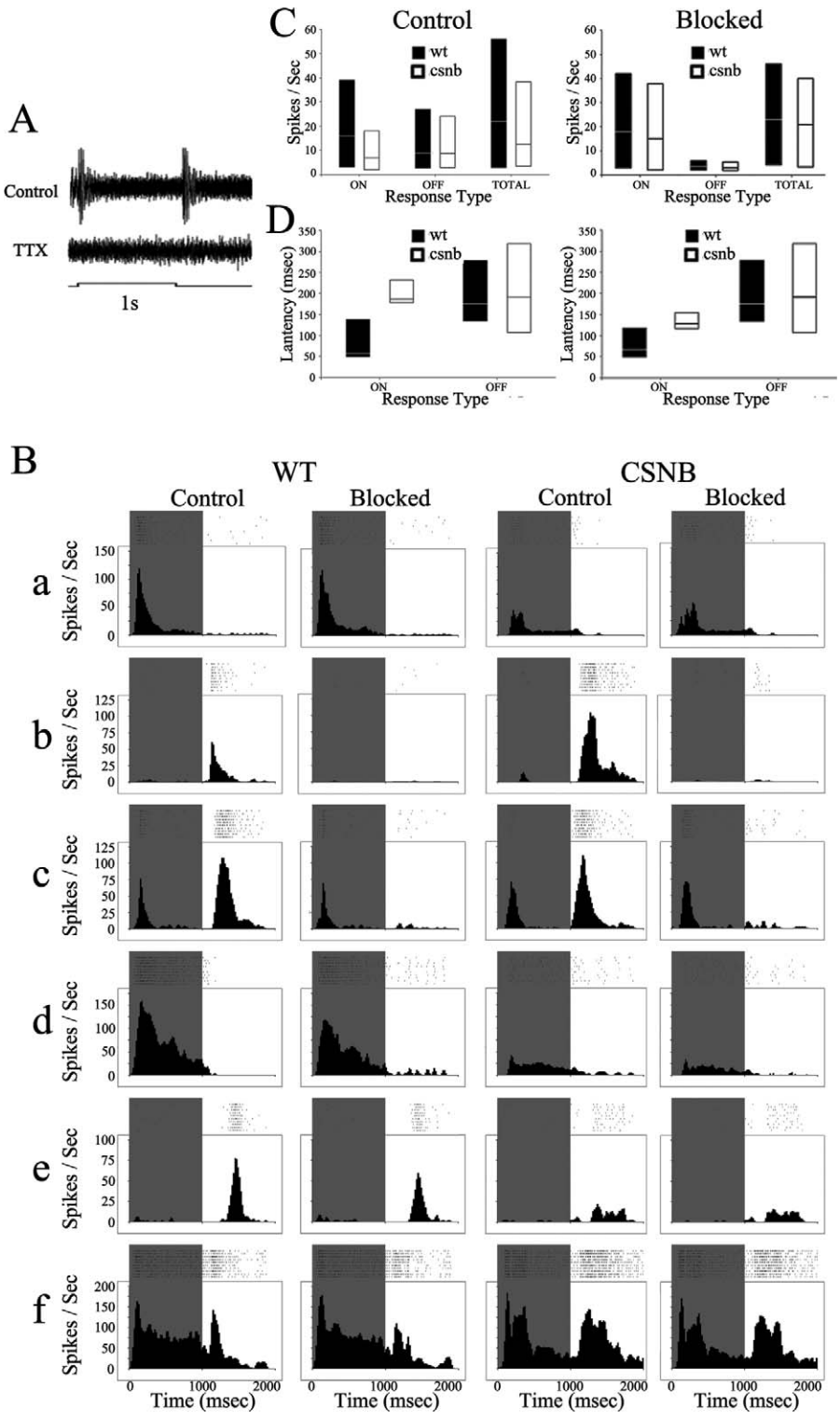

Figure 6. (**A**) The firing spikes were sensitive to TTX and verified our methodologic reliability. (**B**) Raster plots (*up*) of main RGCs populations with corresponding PSTHs: (**a**) ON, (**b**) OFF, (**c**) ON–OFF, (**d**) sustained ON, (**e**) delayed OFF, (**f**) sustained ON–OFF. The CNQX + PDA cocktail was used to block the OFF signal pathway in both Wt and CSNB retinas (Blocked): in both the Wt and the *Cacna1f* mutant retinas, the OFF responses of the OFF RGCs, and the ON–OFF RGCs were disrupted by the blocker, but the OFF response of the delayed OFF RGCs and the sustained ON–OFF RGCs were not. (**C**) The median amplitude of total light-driven response was lower in the *Cacna1f* mutant RGCs than that in the Wt RGCs. This decrease was largely attributed to the aggressive loss of the ON response. After application of the cocktail, the majority of light-induced OFF responses in both the Wt and the CSNB retinas were disrupted; the firing rate of total response decreased, whereas the firing frequency of the ON response increased in the *Cacna1f* mutant retinas. (**D**) The latency was increased significantly for both the OFF and the ON responses in the *Cacna1f* mutant retinas. After application of the cocktail, the latency of the ON responses increased significantly in the *Cacna1f* mutant retinas.

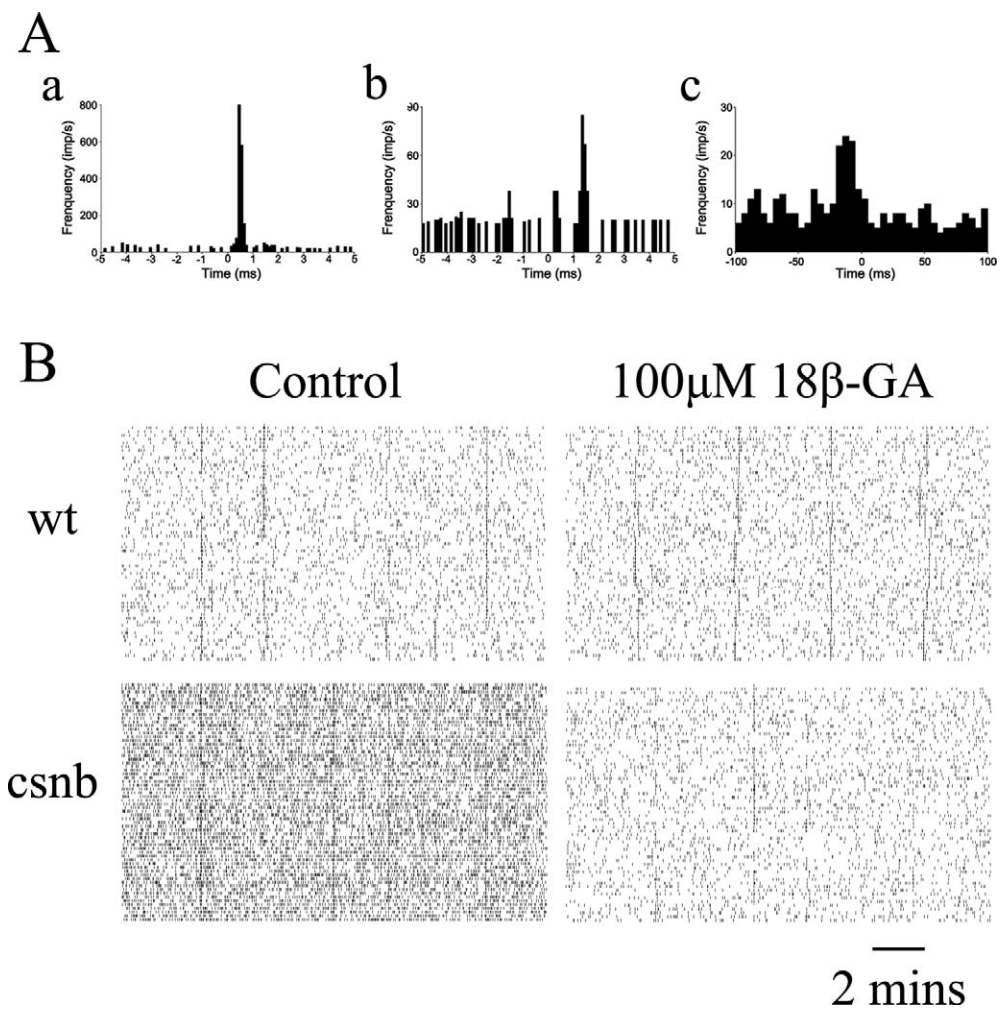

Figure 7. (**A**) The cross-correlations with narrow-scale (<1 ms) correlated activities (**a**) and medium-scale (<25 ms) correlated activities (**b**) were detected in the *Cacna1f* mutant retinas. Another cross-correlation: the broad-scale intervals (40–100 ms) that were common in the Wt retinas (**c**). (**B**) A potent gap junction blocker 18β–GA was applied in the Wt and *Cacna1f* mutated retinas' discharging recordings. In the *Cacna1f* mutated retinas ($n = 5$), 100 μM 18β–GA caused a pronounced decrease in the discharging frequency of spontaneous firing spikes, whereas no appreciated effect was found in any of the Wt retinas ($n = 5$, [**B**]).

findings provide evidence for functional changes that are consistent with retinal network plasticity and remolding after *Cacna1f* mutation. The mechanism of this remolding remains to be known. The altered photoreceptor activity can cause abnormal patterns of synaptic connections in downstream targets.[47–49] The process of switching dendritic connections from rod bipolar cells to cones has been proven to eventually corrupt ON pathways.[30,44] Further immunohistochemical studies are needed to verify if the ectopic synapses in the outer laminae of ONL in *Cacna1f* mutant retinas comply with this rule. Moreover, the OFF pathway is unidirectionaliy inhibited by the ON pathway but not vice versa.[50] Given that the ON pathway, which appears to be more vulnerable to visual signal interruption in the OPL, is severely damaged in the CSNB rats, it is difficult to rule out the possibility that the inhibitory effects of the ON pathway on the OFF RGCs diminished. Another possible explanation is that the decreased excitatory drive of the AII-amacrine (rod) cell may cause disinhibition on the throughput of the OFF-cone bipolar cells.[51]

Analysis of synchronous firing suggests that neighboring RGCs share excitation from the amacrine cells via electrical junctions (medium type), and excite each other cells via electrical junctions (narrow type). Involvement of gap junction transmission in these synchronous RGC discharges implies that the firing patterns in the *Cacna1f* mutant retina are shaped by electrical coupling in the inner retina. It has been reported that some of the gap junction–mediated electrical connections, such as the coupling of AII-amacrine cells and ON-cone bipolar cells within the functional circuits, are vital for retinal plasticity.[52,53] Through the coupling of the AII-amacrine cells and the ON-cone bipolar cells, the rod signals are integrated into the cone pathway and propagate asymmetrically: the rod signals spread into the cone system much more efficiently than the cone signals into the rod system, allowing weak rod signals to be highly amplified and effectively transmitted to the cone system but not vice versa.[54–56] In the *Cacna1f* mutated retinas, the absence of the contribution of broad scale cross-correlation to RGCs' interactions means the vanished polysynaptic inputs from the bipolar cells. Therefore, the malfunction of chemical synaptic inputs from rod bipolar cells to AII-amacrine cells would inevitably affect the downstream electrical correlations between AII-amacrine cells and ON-cone bipolar cells. The asymmetric signal transmission, which amplifies rod signals, is likely to be altered by these dynamic interactions. This rectification might be responsible for the fragility of the rod

signal gain in the *Cacna1f* mutant retinas, and be considered as a novel pathologic theory for the impaired night vision in iCSNB. The paired patch recordings of AII-amacrine cells and ON bipolar cells could be used for quantitative measuring of the rectification of the electrical coupling in the *Cacna1f* mutated retina.[52–55]

Direct evidence for ON/OFF pathway reorganization was identified by pharmacologic experiments. It was shown that the ON pathway in the *Cacna1f* mutant retinas was suppressed by the OFF pathway, and this suppression could be relieved to restore the ON response when the robust OFF pathway was disrupted by the CNQX + PDA cocktail.

These results highlight the importance of understanding how and when malfunction of neurotransmitter release in OPL during early onset CSNB interacts with the visual signal pathway remolding in the downstream inner retinal circuits. Typical physiologic types of the spontaneous and the light-driven response were retained in these retinas, albeit at higher or lower frequencies and with somewhat reorganized patterns than those of the Wt controls. Likewise, synchronous correlation activities recorded from the *Cacna1f* mutant retinas also demonstrated that the basic network interactions in the inner retina are preserved in the absence of chemical synaptic inputs from the outer retina. Together with the partly survived photoreceptor function, these findings ignite the light of hope that visual function could be restored in the *Cacna1f* mutant retinas through gene therapy or cell transplantation, particularly if the treatment or the manipulation of retinal circuit plasticity is timed appropriately.[57,58]

Acknowledgments

The authors thank personnel from the Institute for Biomedical Sciences of Pain (IBSP) of the Fourth Military Medical University for technical support.

References

1. Lasater EM. Membrane currents of retinal bipolar cells in culture. *J Neurophysiol*. 1988;60:1460–1480.
2. Singer JH, Diamond JS. Vesicle depletion and synaptic depression at a mammalian ribbon synapse. *J Neurophysiol*. 2006;95:3191–3198.
3. Protti DA, Llano I. Calcium currents and calcium signaling in rod bipolar cells of rat retinal slices. *J Neurosci*. 1998;18:3715–3724.
4. Rouze NC, Schwartz EA. Continuous and transient vesicle cycling at a ribbon synapse. *J Neurosci*. 1998;18:8614–8624.
5. von Gersdorff H, Matthews G. Dynamics of synaptic vesicle fusion and membrane retrieval in synaptic terminals. *Nature*. 1994;367:735–739.
6. von Gersdorff H, Matthews G. Depletion and replenishment of vesicle pools at a ribbon-type synaptic terminal. *J Neurosci*. 1997;17:1919–1927.
7. von Gersdorff H, Matthews G. Electrophysiology of synaptic vesicle cycling. *Annu Rev Physiol*. 1999;61:725–752.
8. McRory JE, Hamid J, Doering CJ, et al. The CACNA1F gene encodes an L-type calcium channel with unique biophysical properties and tissue distribution. *J Neurosci*. 2004;24:1707–1718.
9. Hemara-Wahanui A, Berjukow S, Hope CI, et al. A CACNA1F mutation identified in an X-linked retinal disorder shifts the voltage dependence of Cav1.4 channel activation. *Proc Natl Acad Sci U S A*. 2005;102:7553–7558.
10. Mansergh F, Orton NC, Vessey JP, et al. Mutation of the calcium channel gene Cacna1f disrupts calcium signaling, synaptic transmission and cellular organization in mouse retina. *Hum Mol Genet*. 2005;14:3035–3046.
11. Boycott KM, Maybaum TA, Naylor MJ, et al. A summary of 20 CACNA1F mutations identified in 36 families with incomplete X-linked congenital stationary night blindness, and characterization of splice variants. *Hum Genet*. 2001;108:91–97.
12. Zhang Z, Gu Y, Li L, Long T, Guo Q, Shi L. A potential spontaneous rat model of X-linked congenital stationary night blindness. *Doc Ophthalmol*. 2003;107:53–57.
13. Chang B, Heckenlively JR, Bayley PR, et al. The nob2 mouse, a null mutation in Cacna1f: anatomical and functional abnormalities in the outer retina and their consequences on ganglion cell visual responses. *Vis Neurosci*. 2006;23:11–24.
14. Bayley PR, Morgans CW. Rod bipolar cells and horizontal cells form displaced synaptic contacts with rods in the outer nuclear layer of the nob2 retina. *J Comp Neurol*. 2007;500:286–298.
15. Gu Y, Wang L, Zhou J, et al. A naturally-occurring mutation in Cacna1f in a rat model of congenital stationary night blindness. *Mol Vis*. 2008;14:20–28.
16. Miyake Y, Yagasaki K, Horiguchi M, Kawase Y, Kanda T. Congenital stationary night blindness with negative electroretinogram. A new classification. *Arch Ophthalmol*. 1986;104:1013–1020.
17. Zheng L, Yan Y, An J, et al. Retinal horizontal cells reduced in a rat model of congenital stationary night blindness. *Neurosci Lett*. 2012;521:26–30.
18. Stett A, Egert U, Guenther E, et al. Biological application of microelectrode arrays in drug discovery and basic research. *Anal Bioanal Chem*. 2003;377:486–495.
19. Chen AH, Zhou Y, Gong HQ, Liang PJ. Firing rates and dynamic correlated activities of ganglion cells both contribute to retinal information processing. *Brain Res*. 2004;1017:13–20.
20. Segev R, Goodhouse J, Puchalla J, Berry MN. Recording spikes from a large fraction of the ganglion cells in a retinal patch. *Nat Neurosci*. 2004;7:1154–1161.
21. Kolomiets B, Dubus E, Simonutti M, Rosolen S, Sahel JA, Picaud S. Late histological and functional changes in the P23H rat retina after photoreceptor loss. *Neurobiol Dis*. 2010;38:47–58.
22. Busskamp V, Duebel J, Balya D, et al. Genetic reactivation of cone photoreceptors restores visual responses in retinitis pigmentosa. *Science*. 2010;329:413–417.
23. Zhou Y, Liu X, Liang PJ. The dual-peak light response of ganglion cells in chicken retina. *Brain Res*. 2007;1138:104–110.
24. Homma K, Osakada F, Hirami Y, Jin ZB, Mandai M, Takahashi M. Detection of localized retinal malfunction in retinal degeneration model using a multielectrode array system. *J Neurosci Res*. 2009;87:2175–2182.
25. Ryu SB, Ye JH, Lee JS, Goo YS, Kim CH, Kim KH. Electrically-evoked neural activities of rd1 mice retinal ganglion cells by repetitive pulse stimulation. *Korean J Physiol Pharmacol*. 2009;13:443–448.
26. Jensen RJ, Ziv OR, Rizzo JF. Responses of rabbit retinal ganglion cells to electrical stimulation with an epiretinal electrode. *J Neural Eng*. 2005;2:S16–S21.
27. Ryu SB, Ye JH, Lee JS, Goo YS, Kim KH. Characterization of retinal ganglion cell activities evoked by temporally patterned electrical stimulation for the development of stimulus encoding strategies for retinal implants. *Brain Res*. 2009;1275:33–42.
28. Fedrowitz M, Lindemann S, Loscher W, Gernert M. Altered spontaneous discharge rate and pattern of basal ganglia output neurons in the circling (ci2) rat mutant. *Neuroscience*. 2003;118:867–878.

29. Kononenko NI, Dudek FE. Mechanism of irregular firing of suprachiasmatic nucleus neurons in rat hypothalamic slices. *J Neurophysiol*. 2004;91:267–273.
30. Stasheff SF. Emergence of sustained spontaneous hyperactivity and temporary preservation of OFF responses in ganglion cells of the retinal degeneration (rd1) mouse. *J Neurophysiol*. 2008; 99:1408–1421.
31. Sagdullaev BT, McCall MA. Stimulus size and intensity alter fundamental receptive-field properties of mouse retinal ganglion cells in vivo. *Vis Neurosci*. 2005;22:649–659.
32. Schnitzer MJ, Meister M. Multineuronal firing patterns in the signal from eye to brain. *Neuron*. 2003;37:499–511.
33. Brivanlou IH, Warland DK, Meister M. Mechanisms of concerted firing among retinal ganglion cells. *Neuron*. 1998; 20:527–539.
34. Sillman AJ, Ito H, Tomita T. Studies on the mass receptor potential of the isolated frog retina. I. General properties of the response. *Vision Res*. 1969;9:1435–1442.
35. Pepperberg DR, Masland RH. Retinal-induced sensitization of light-adapted rabbit photoreceptors. *Brain Res*. 1978;151: 194–200.
36. Brown KT, Watanabe K. Isolation and identification of a receptor potential from the pure cone fovea of the monkey retina. *Nature*. 1962;193:958–960.
37. Nilsson SE. Human retinal vascular obstructions. A quantitative correlation of angiographic and electroretinographic findings. *Acta Ophthalmol (Copenh)*. 1971;49:111–133.
38. Hood DC, Frishman LJ, Viswanathan S, Robson JG, Ahmed J. Evidence for a ganglion cell contribution to the primate electroretinogram (ERG): effects of TTX on the multifocal ERG in macaque. *Vis Neurosci*. 1999;16:411–416.
39. Robson JG, Frishman LJ. Dissecting the dark-adapted electroretinogram. *Doc Ophthalmol*. 1998;95:187–215.
40. Kuffler SW. Discharge patterns and functional organization of mammalian retina. *J Neurophysiol*. 1953;16:37–68.
41. Drager UC, Hubel DH. Studies of visual function and its decay in mice with hereditary retinal degeneration. *J Comp Neurol*. 1978;180:85–114.
42. Sauve Y, Girman SV, Wang S, Lawrence JM, Lund RD. Progressive visual sensitivity loss in the Royal College of Surgeons rat: perimetric study in the superior colliculus. *Neuroscience*. 2001;103:51–63.
43. Pu M, Xu L, Zhang H. Visual response properties of retinal ganglion cells in the Royal College of Surgeons dystrophic rat. *Invest Ophthalmol Vis Sci*. 2006;47:3579–3585.
44. Stasheff SF, Shankar M, Andrews MP. Developmental time course distinguishes changes in spontaneous and light-evoked retinal ganglion cell activity in rd1 and rd10 mice. *J Neurophysiol*. 2011;105:3002–3009.
45. Wong WT, Wong RO. Changing specificity of neurotransmitter regulation of rapid dendritic remodeling during synaptogenesis. *Nat Neurosci*. 2001;4:351–352.
46. Cuenca N, Pinilla I, Sauve Y, Lund R. Early changes in synaptic connectivity following progressive photoreceptor degeneration in RCS rats. *Eur J Neurosci*. 2005;22:1057–1072.
47. Hooks BM, Chen C. Distinct roles for spontaneous and visual activity in remodeling of the retinogeniculate synapse. *Neuron*. 2006;52:281–291.
48. Demas J, Sagdullaev BT, Green E, et al. Failure to maintain eye-specific segregation in nob, a mutant with abnormally patterned retinal activity. *Neuron*. 2006;50:247–259.
49. Haeseleer F, Imanishi Y, Maeda T, et al. Essential role of Ca2+-binding protein 4, a Cav1.4 channel regulator, in photoreceptor synaptic function. *Nat Neurosci*. 2004;7:1079–1087.
50. Renteria RC, Tian N, Cang J, Nakanishi S, Stryker MP, Copenhagen DR. Intrinsic ON responses of the retinal OFF pathway are suppressed by the ON pathway. *J Neurosci*. 2006; 26:11857–11869.
51. Taylor WR, Smith RG. Transmission of scotopic signals from the rod to rod-bipolar cell in the mammalian retina. *Vision Res*. 2004;44:3269–3276.
52. Veruki ML, Hartveit E. Electrical synapses mediate signal transmission in the rod pathway of the mammalian retina. *J Neurosci*. 2002;22:10558–10566.
53. Pang JJ, Abd-El-Barr MM, Gao F, Bramblett DE, Paul DL, Wu SM. Relative contributions of rod and cone bipolar cell inputs to AII amacrine cell light responses in the mouse retina. *J Physiol*. 2007;580:397–410.
54. Pang JJ, Gao F, Wu SM. Light-evoked current responses in rod bipolar cells, cone depolarizing bipolar cells and AII amacrine cells in dark-adapted mouse retina. *J Physiol*. 2004;558:897–912.
55. Wu SM. From retinal circuitry to eye diseases—in memory of Henk Spekreijse. *Vision Res*. 2009;49:992–995.
56. Yang XL. Characterization of receptors for glutamate and GABA in retinal neurons. *Prog Neurobiol*. 2004;73:127–150.
57. Lev S. Molecular aspects of retinal degenerative diseases. *Cell Mol Neurobiol*. 2001;21:575–589.
58. Fritz JJ, Lewin A, Hauswirth W, Agarwal A, Grant M, Shaw L. Development of hammerhead ribozymes to modulate endogenous gene expression for functional studies. *Methods*. 2002; 28:276–285.